

# Adaptive Radome Compensation Using Dither

Paul Zarchan\*

*Charles Stark Draper Laboratory, Inc., Cambridge, Massachusetts 02139*

and

Harvey Gratt†

*Missile Systems and Technologies, Inc., Huntsville, Alabama 35814*

**A** technique is presented for estimating a radar homing missile's radome slope by the use of a nondestructive dither signal on the acceleration command. A planar example is presented in detail showing how bandpass filtering is used to extract the radome slope estimate and then to compensate for unwanted radome aberration angle effects. A second example is presented showing how Kalman filtering techniques can also be used for the same planar example to estimate the radome slope. Although the Kalman filter approach does not yield superior radome slope estimates, it does provide a solid framework so that the radome slope estimation technique can be extended to the more realistic three-dimensional case where cross-plane slopes are important.

## Introduction

ALL endoatmospheric radar homing missiles have a radome at the front end to protect the missile seeker from the airflow. In addition to being durable, the radome must also allow the incoming signal, i.e., reflected energy off the target, to be passed without too much attenuation or distortion. However, because the incoming signal is passing through several different media, a refraction or bending of the signal takes place before it reaches the seeker, which in turn causes a false indication of the target location. The false target location indication causes the missile flight control system to respond in the wrong way, i.e., missile goes up when it should go down and vice versa. In other words, the radome refraction effect is destabilizing to the missile guidance system. The stability problem becomes more severe as the interceptor engagement altitude increases.

One approach for alleviating the radome refraction problem is to increase the missile guidance system time constant. Although this technique is easy to implement, it tends to increase the miss distance over that which could be achieved at the lower altitudes where the guidance system time constant is smaller. A more popular technique for alleviating the radome refraction problem is by using compensation tables stored in the missile flight computer. In this case, a representative radome is measured or mapped extensively in an anechoic chamber, and the resulting measurements are stored in the missile's flight computer to compensate in flight for radome refraction effects. The effectiveness of the technique depends on the accuracy of the measurements, i.e., radome aberration angle. Significant degradation may take place if the test radome differs significantly from the flight radome or if the radomes electrical characteristics are not the same at room temperature, i.e., where the measurements are taken, as they are in flight.<sup>1</sup> Traditionally, the radome issue has limited the high-altitude performance of all radar-guided aerodynamically controlled missiles.

The purpose of this paper is to suggest a way of alleviating the radome refraction problem, which in turn would improve the high-altitude performance of the interceptor. It will be shown that the radome slope (important parameter related to radome aberration angle) can be estimated quickly during the missile flight by using a dither signal and simple bandpass filtering to extract useful information. Knowledge of the radome slope leads to a determination of the radome aberration angle, which in turn can be used to com-

pen-  
sate for the actual unwanted aberration angle that contaminates the guidance signal.

A simplified planar example is presented illustrating adaptive radome compensation for the case in which the radome slope is constant. It is recognized that extensive modifications would have to be made to the adaptive radome estimation technique described to the more realistic case where the slope is not constant and cross-plane slopes are also present. However, it is also believed that the step by step approach taken suggests ways and provides a practical engineering framework in which the more complex problem can be addressed.

## Minimum Guidance System Time Constant

References 2 and 3 show that the radome aberration effects create an unwanted feedback path in the missile guidance system, which can cause stability problems. Figure 1 presents a block diagram of a simplified fifth-order binomial proportional navigation guidance system with radome effects included. In this diagram, missile acceleration  $n_L$  is subtracted from target acceleration  $n_T$  to form a relative acceleration. After two integrations, we have relative position, which at the end of the flight is the miss distance  $y(t_F)$ . A division by range  $R_{TM}$  yields the geometric line-of-sight angle  $\lambda$ .

The missile seeker, which is represented in Fig. 1 as a first-order filter with a derivative in the numerator, attempts to track the target. Effectively, the seeker is taking the derivative of the noise contaminated geometric line-of-sight angle, thus providing a noisy measurement of the line-of-sight rate. The noise filter, which is represented in Fig. 1 as a single-pole low-pass filter, must process the seeker measurement and provide a smoothed estimate of the line-of-sight rate. A guidance command  $n_c$  is generated, based on the proportional navigation guidance law, from the noise filter output. Because the interceptor acceleration capability is finite, the acceleration command is limited to acceleration value  $n_{lim}$ . In tactical aerodynamically controlled missiles, the flight control system, which is represented as a third-order transfer function in Fig. 1 (two time constants for the aerodynamics and one time constant for the autopilot), must by moving control surfaces cause the missile to maneuver in such a way that the achieved acceleration matches the desired acceleration.

The important elements in the unwanted feedback path due to radome slope effects have been shaded in Fig. 1. The key parameters in radome analysis are the missile turning rate time constant  $T_\alpha$ , the radome slope  $R$ , and the missile velocity  $V_M$ . The turning rate time constant is a measure of the time it takes to turn the missile flight-path angle through an equivalent angle of attack. Larger values of turning rate time constant tend to exacerbate the radome problem. The turning rate time constant increases with increasing altitude and decreasing missile velocity. Therefore, the radome problem becomes especially important at the higher altitudes.

Presented as Paper 96-3879 at the AIAA Guidance, Navigation, and Control Conference, San Diego, CA, July 29–31, 1996; received Dec. 24, 1996; revision received Aug. 27, 1998; accepted for publication Aug. 28, 1998. Copyright © 1998 by the American Institute of Aeronautics and Astronautics, Inc. All rights reserved.

\*Principal Member of Technical Staff, Guidance and Navigation Department, Associate Fellow AIAA.

†Consultant, Member AIAA.

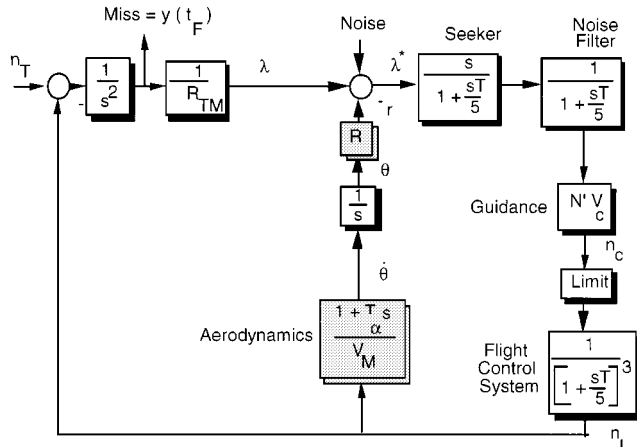


Fig. 1 Model of guidance system with radome effects.

The radome refraction or aberration angle  $r$  varies with the missile look angle  $\lambda - \theta$  (line-of-sight angle minus missile body angle). The radome slope is defined as the rate of change of the aberration angle with the look angle or

$$R = \frac{dr}{d(\lambda - \theta)}$$

Although the radome slope varies during a flight it is often convenient to think of the slope as a constant. Often radomes are characterized by their largest negative and positive slope values. Large positive or negative slope values tend to exacerbate the guidance system stability problem.

In the presence of radome slope, the missile guidance system transfer function can be derived from Fig. 1, i.e., neglecting acceleration saturation effects, and can be shown to be given by

$$\frac{n_L}{\lambda} = \frac{N' V_c}{[1 + (sT/5)]^5 + (N' V_c R/V_M)(1 + T_\alpha s)}$$

where  $T$  is the guidance system time constant. We can see from the preceding equation that if the radome slope is zero the guidance system transfer function reduces to a fifth-order binomial. One can show mathematically<sup>2,3</sup> that if the ratio of the turning rate time constant to the guidance system time constant is greater than unity or

$$T_\alpha/T > 1$$

then the guidance system transfer will be stable only if the following inequality is satisfied:

$$-0.79 < \frac{N' V_c R T_\alpha}{V_M T} < 2.07$$

Therefore, if the radome slope is negative, we can find from the preceding inequality that the minimum guidance system time constant to yield a stable guidance system is given by

$$T_{\min} = \frac{N' V_c R T_\alpha}{0.79 V_M}$$

whereas for positive radome slopes the minimum guidance system time constant to yield a stable guidance system turns out to be

$$T_{\min} = \frac{N' V_c R T_\alpha}{2.07 V_M}$$

We can see from the preceding relationships that engagements with larger closing velocities, i.e., ballistic targets, or those taking place at high altitudes, i.e., larger turning rate time constant, will require a larger missile guidance system time constant to keep the guidance system stable. However, as already mentioned, the larger guidance system time constants will also tend to increase the miss distance.

Table 1 Guidance system parameters

Name	Symbol	Value
Guidance system time constant	$T$	0.3 s
Turning rate time constant	$T_\alpha$	5 s
Missile velocity	$V_M$	4000 ft/s
Closing velocity	$V_c$	6000 ft/s
Effective navigation ratio	$N'$	3
Missile acceleration limit	$n_{\lim}$	20 g

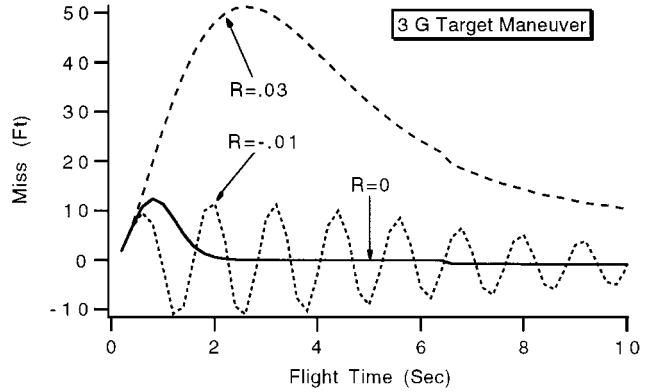


Fig. 2 Positive and negative radome slope can degrade system performance.

To check the preceding formulas, several simulation experiments were conducted using the value of the various guidance system parameters shown Table 1.

Using the values of Table 1 and the preceding formulas we can see that a minimum guidance system time constant of 0.28 s is required for a negative radome slope of  $-0.01$  and  $0.32$  s for a positive radome slope of  $0.03$ . Figure 2 shows from a simulation point of view how the miss due to a 3-g step target maneuver varies with flight time for radome slope values of  $-0.01$ ,  $0.03$ , and  $0$ , respectively, when the missile guidance system time constant is  $0.3$  s. We can see from Fig. 2 that the miss is quite large for the positive radome slope, is oscillatory for the negative radome slope, and is small and well behaved for zero radome slope, thus confirming the theoretical formulas for the minimum guidance system time constant. The goal of adaptive radome estimation will be to improve both the negative and positive radome slope performance of the guidance system. If the radome slope can be accurately estimated, then compensation techniques can be used at higher altitudes to improve overall system performance.

### Bandpass Filters

Bandpass filters are well known in signal processing and can be used to extract a sinusoidal signal of known frequency that is embedded in noise. One set of such filters has the transfer function

$$H(s) = \frac{K s^n}{(1 + s/\omega_0)^{2n}} \quad n = 1, 2, 3, \dots$$

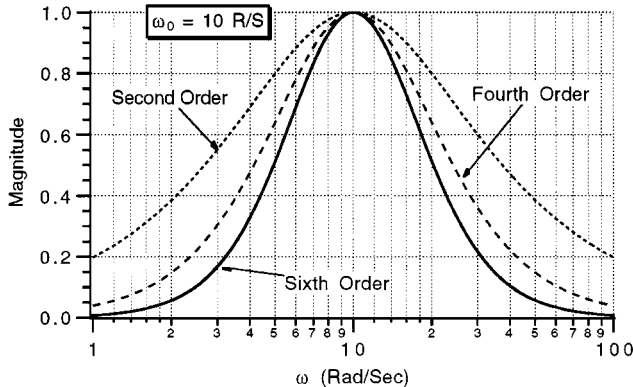
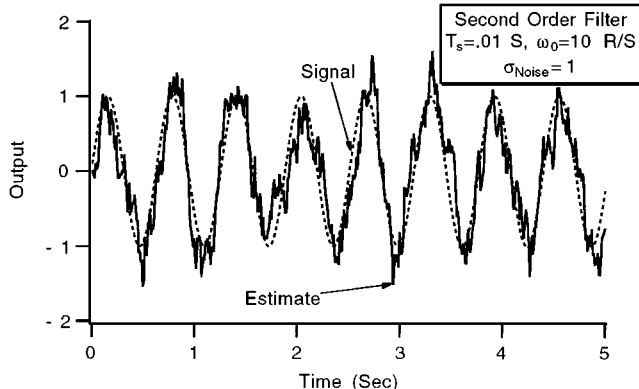
where  $2n$  determines the filter order and the gain  $K$  can be chosen to provide unity transmission at the bandpass filter natural frequency  $\omega_0$ .

It is often easier to understand bandpass filter properties in the complex frequency domain, i.e., replace  $s$  with  $j\omega$ . Table 2 presents second-, fourth-, and sixth-order bandpass filters transfer functions in the Laplace transform domain and the magnitude of the transfer function in the complex frequency domains. The gain  $K$  for each of the filters has been chosen to provide unity transmission at the bandpass filter natural frequency  $\omega_0$ .

The magnitudes of the different order bandpass filters are shown in Fig. 3. We can first see that all filters have unity magnitude at  $10$  rad/s, i.e., the bandpass filter natural frequency in this example. Next we can see that as the filter order increases, the amount of attenuation at frequencies other than the natural frequency increases. For example, at  $5$  rad/s the magnitude of the bandpass filter transfer function is approximately  $0.8$  for a second-order filter,  $0.6$  for a

**Table 2 Transfer functions and magnitudes of several bandpass filters**

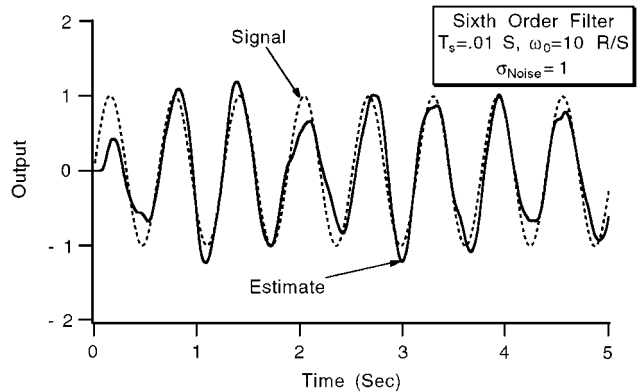
Name	Laplace transform	Magnitude
Second order	$H(s) = \frac{2s}{\omega_0[1 + (s/\omega_0)]^2}$	$ H(j\omega)  = \frac{2\omega}{\omega_0[1 + (\omega^2/\omega_0^2)]}$
Fourth order	$H(s) = \frac{4s^2}{\omega_0^2[1 + (s/\omega_0)]^4}$	$ H(j\omega)  = \frac{4\omega^2}{\omega_0^2[1 + (\omega^2/\omega_0^2)]^2}$
Sixth order	$H(s) = \frac{8s^3}{\omega_0^3[1 + (s/\omega_0)]^6}$	$ H(j\omega)  = \frac{8\omega^3}{\omega_0^3[1 + (\omega^2/\omega_0^2)]^3}$

**Fig. 3 Higher-order bandpass filters have better rejection properties.****Fig. 4 Low-order bandpass filter can remove signal from noise.**

fourth-order filter, and 0.5 for a sixth-order filter. In other words, the filter is becoming more selective as the filter order increases. In the limit, the ideal bandpass filter should have magnitude of unity at 10 rad/s and magnitude zero everywhere else.

To illustrate some fundamental properties of bandpass filters, an experiment was conducted in which a 10r/s sinusoidal signal of unity amplitude was corrupted by Gaussian noise with standard deviation of one every 0.01 s. In this case, the signal to noise ratio was one. Figure 4 shows that when this noisy measurement is passed through a second-order bandpass filter the output is a noisy version of the input. We can see that although the bandpass filter output is of the same frequency as the noise-free input signal, the output is rather jagged. In other words, some of the noise has not been rejected by the low-order bandpass filter.

Figure 5 shows that when a higher-order bandpass filter is used more of the noise is rejected and the filter output more closely resembles the input signal before it is contaminated by noise. However, by comparing Figs. 4 and 5, we can see that a higher-order filter also requires a longer initial time to get good estimates than the lower-order filter. In other words, the transient properties of this type of bandpass filter will degrade as the filter order increases. Normally, this phenomenon is of no concern in the signal processing world where frequencies are in the megahertz regime, but will be of concern to the guidance system engineer where frequencies of interest

**Fig. 5 Higher-order filter does better job of rejecting noise.**

are a million times smaller. Because the eventual application of the bandpass filter will be a missile guidance system where time constant issues are very important, we will not consider bandpass filters higher than sixth order.

### Using Dither to Estimate Radome Slope

Several investigators have reported success in using banks of Kalman filters, each tuned differently, to estimate radome slope.<sup>4,5</sup> In this paper, a simpler and less computationally intensive approach is taken, where a dither signal and bandpass filtering are used to adaptively estimate the radome slope. The idea behind using a dither signal for estimation purposes is certainly not new and has been used by many including Stallard<sup>6</sup> and Gratt.<sup>1</sup> Stallard applied the dithering concept to an autopilot design application, whereas Gratt applied dithering to the radome estimation problem. Many experienced engineers also know that in the 1960s and 1970s there were undocumented, unsuccessful attempts in applying dithering to the radome problem. Although the lack of documentation prevents one from knowing why these attempts failed, one possibility could be the large amount of seeker noise present. The proposed scheme will deteriorate if there is an order of magnitude more noise. There is much less seeker noise today than there was several decades ago because of hardware improvements. In addition, many seekers now operate at higher frequencies, which further reduces the noise.

In the proposed scheme a dither signal of fixed amplitude and frequency is added to the proportional navigation acceleration command. The amplitude of the dither signal is chosen to be small enough and the frequency high enough so that the known disturbance or intentional guidance system bias will not cause additional miss distance. In other words, we are attempting to add a nondestructive signal of known frequency and amplitude to the guidance system.

If the missile guidance system is assumed to be operating in the nearly linear region, i.e., not in acceleration saturation, the missile body angle  $\theta$  (which can be obtained from seeker dish and gimbal angle measurements) and measured line-of-sight angle  $\lambda^*$  (which can be obtained from seeker dish angle and boresight error measurements) will also have an attenuated signal component due to a dither signal applied at the acceleration command. If we bandpass filter the line-of-sight angle measurement and divide it by the negative of the bandpass filtered body angle measurement we can obtain an estimate of the radome slope.

To test this simple dithering concept, an experiment was conducted in which a noise-free 10-s flight was investigated in which the only disturbance was a 3-g target maneuver. The sinusoidal dither amplitude was 3 g, whereas the dither frequency was 10 rad/s. The actual radome slope considered for the experiment was -0.01. The radome estimation scheme described in the preceding paragraph was slightly modified so that if the denominator in the division required to estimate radome slope was zero the slope estimate would be set to zero. In addition, slope estimates would be automatically limited to maximum and minimum values, i.e.,  $\pm 0.06$  in this example, to represent a priori knowledge of radome physics. In other words, we already know maximum and minimum radome slope values from radome acceptance tests.

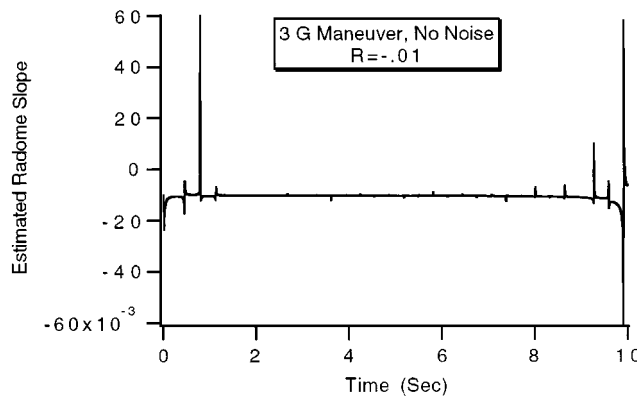


Fig. 6 Dithering can be used to estimate negative radome slope.

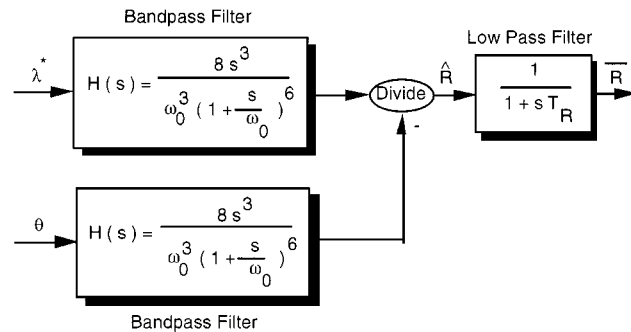


Fig. 7 Low-pass filter can be used to smooth radome estimates.

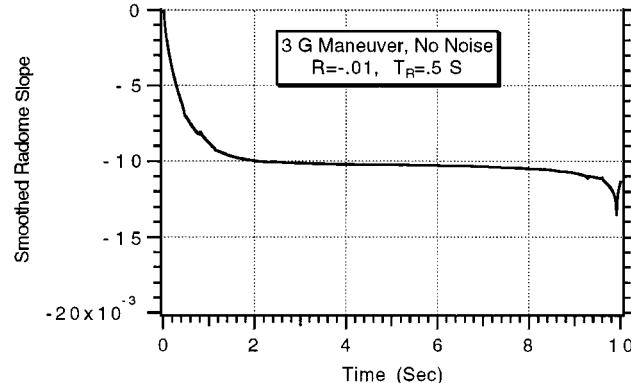


Fig. 8 Estimated radome slope spikes are eliminated by 0.5-s low-pass filter.

Figure 6 shows that in the presence of the target maneuver disturbance the estimated slope is very near the true value of  $-0.01$ . However, Fig. 6 also shows that there are several spikes in the radome slope estimates, which are fortunately limited to  $\pm 0.06$ .

The spikes of the radome slope estimates are undesirable and can be removed by common sense, i.e., by editing the data, or smoothed by low-pass filtering. Figure 7 shows how a single-pole low-pass filter can be implemented to get a smoothed radome slope estimate.

The same case of Fig. 6 was repeated, except this time a 0.5-s, i.e.,  $T_R = 0.5$  s, low-pass filter was used to smooth the radome estimates. Figure 8 demonstrates that the low-pass filter eliminates the spikes from the radome estimate. In addition, we can see that the slope estimate is nearly equal to the true value of  $-0.01$ .

### Radome Slope Estimation and Miss Distance

To make effective use of the smoothed radome slope estimate in the missile guidance system, we multiply the radome slope estimate by the measured body angle to obtain an estimate of the aberration angle. The estimated aberration angle is added to the measured line-of-sight angle  $\lambda^*$  in attempt to cancel out the existing, unwanted aberration angle, as shown in the block diagram of Fig. 9.

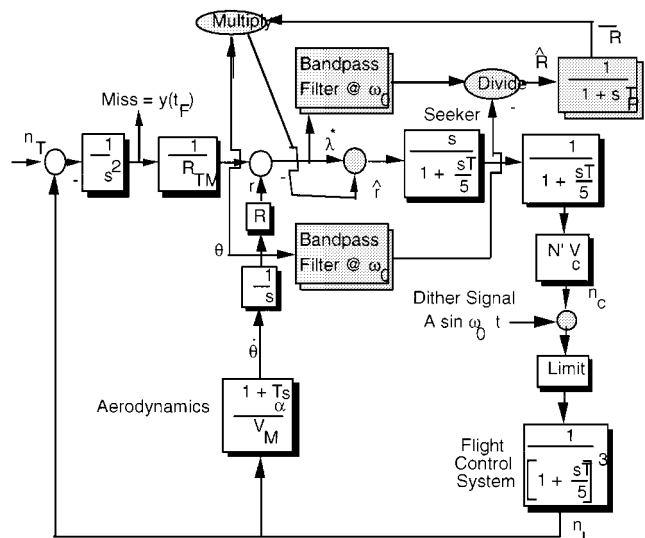


Fig. 9 Incorporating radome slope estimation in homing loop.

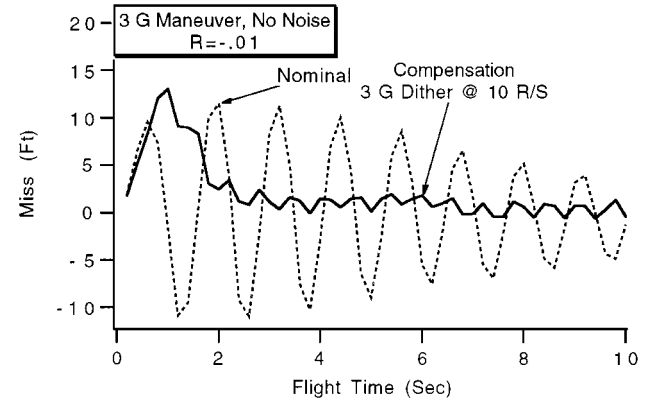


Fig. 10 Compensation reduces miss due to negative radome slope.

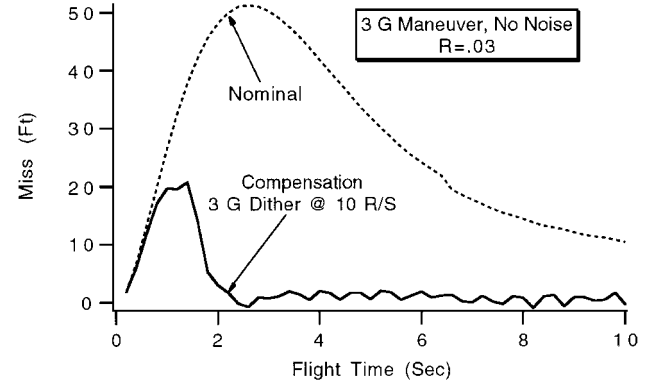


Fig. 11 Compensation reduces miss due to positive radome slope.

Miss distance experiments were conducted for the case in which the disturbance was a 3-g target maneuver initiated at the beginning of the engagement for various flight times. Figures 10 and 11 show that, in general, the miss due to negative and positive radome slope effects is dramatically improved when adaptive radome compensation is used with a 3-g, 10-rad/s dither signal. Only when the flight time is short does radome compensation lose its effectiveness. The reason for the loss of effectiveness is that the frequency of the dither signal is not high enough relative to the short flight time to ensure that the dither signal is nondestructive.

### How Measurement Noise Influences Performance

So far all of the results presented have been in a noise-free environment. The purpose of this section is to determine how measurement

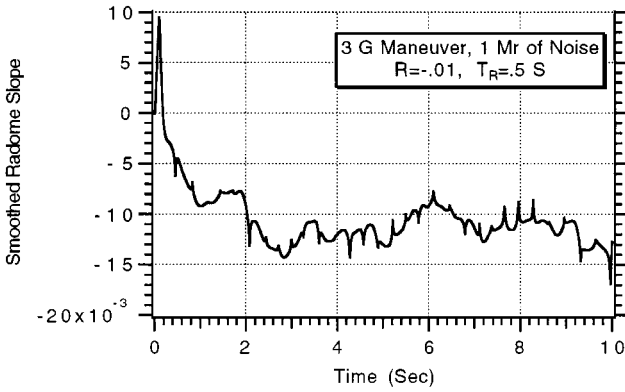


Fig. 12 Measurement noise slightly degrades radome slope estimates.

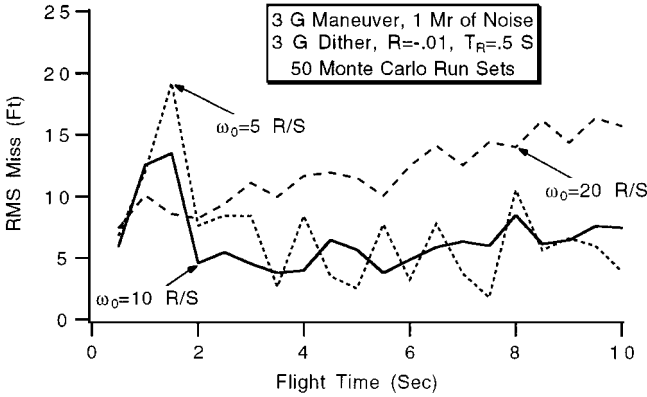


Fig. 13 Higher dither frequencies are not as effective in presence of measurement noise.

noise degrades the results presented so far. Consider a case in which there is 1 mrad of measurement noise entering the guidance system every 0.01 s on the line-of-sight angle. In addition, we will still assume that the sinusoidal dither signal is 3 g at 10 rad/s. Figure 12 presents single-flight results, which indicate that although the estimated radome slope is noisier than it was before it is still very close to the true value of  $-0.01$ .

Rather than just present more radome slope estimate results, consider the entire guidance system and investigate how the rms miss distance due to target maneuver and noise depends on the dither signal frequency. In this example, the dither amplitude is fixed at 3 g. Figure 13 indicates that going to higher dither frequencies, i.e., nominal dither frequency is considered to be 10 rad/s, increases the rms miss distance because less noise is being rejected by the bandpass filters. We can see that going to smaller dither frequencies increases the rms miss for short flight times because the dither signal frequency is near the guidance system bandwidth. For this example, it appears that 10 rad/s is a good choice for the dither frequency.

In all of the experiments conducted so far, the dither amplitude has been set to 3 g. In the next experiment the dither frequency is set to 10 rad/s, and the dither amplitude is varied. Figure 14 shows that the rms miss due to both target maneuver and measurement noise improves as the dither amplitude increases and gets worse if the dither amplitude decreases. Larger dither amplitudes make it easier to estimate the radome slope because it is more observable. For future work we will keep the dither amplitude fixed at 3 g.

More filtering could have been done on the raw estimated slopes to get the smoothed radome slopes. Figure 15 shows that the rms miss distance results improve if the low-pass filter time constant  $T_R$  increases from the nominal value of 0.5 to 1 s. However, in reality, the radome slope will not be a constant throughout the flight and so a small value of low-pass filter time constant is desirable. Therefore, future results will use the nominal value of 0.5 s for the time constant.

To see the true benefits of radome compensation, it is best to make comparisons with cases in which there is no radome compensation at all. Figure 16 shows how the rms miss due to target maneuver

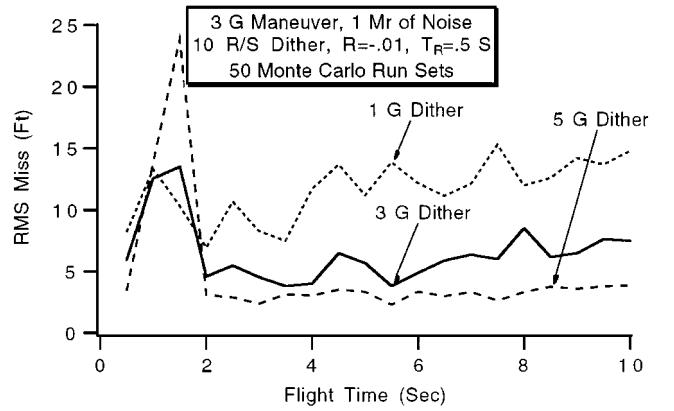


Fig. 14 Performance improves when dither amplitude increases.

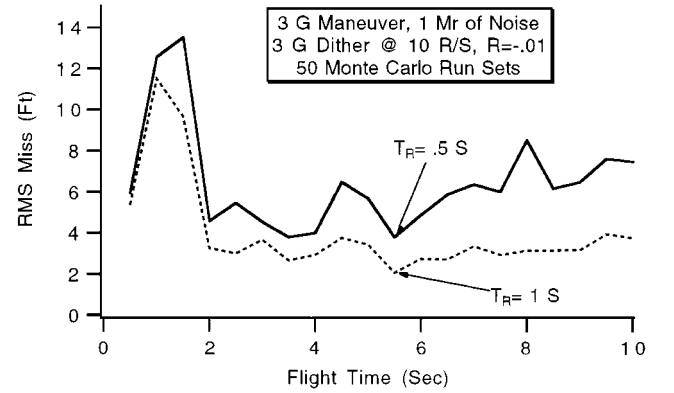


Fig. 15 Increasing time constant for smoothing improves performance.

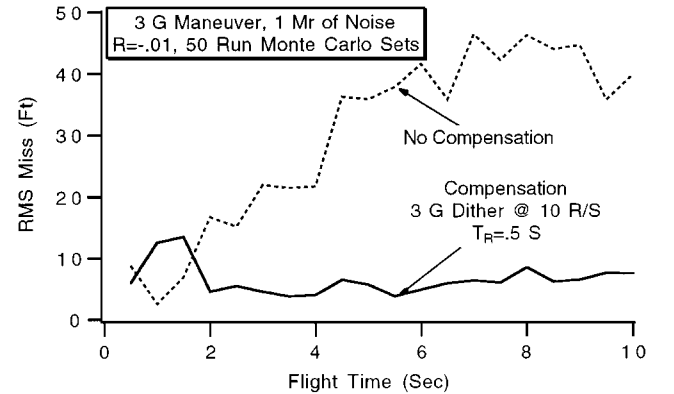


Fig. 16 Radome compensation in presence of noise is beneficial for negative radome slopes.

and measurement noise varies with flight time for a negative radome slope. Note that in both cases adaptive radome compensation dramatically reduces the rms miss distance.

So far all of the experiments conducted have assumed a 3-g target maneuver and 1 mrad of measurement noise. It is appropriate to ask if the adaptive radome compensation scheme would break down or degrade if either the target maneuver level or measurement noise level increased. To conduct the experiment, the missile acceleration limit was increased from 20 to 30 g so that the missile would still be operating in the linear region with the increased level of the error sources. Figure 17 shows that increasing the target maneuver level from 3 to 5 g does not effect the radome slope estimates.

At high altitudes it may not be possible to have a 3-g dither because of angle-of-attack constraints. However, in this case there would also probably not be a 3-g target maneuver, i.e., a slower traveling aircraft will have significantly less maneuverability than a missile at the same altitude. The results of this section were checked in two ways. First, key cases were repeated in which there was a 3-g target maneuver and 1-g dither. In those experiments the miss

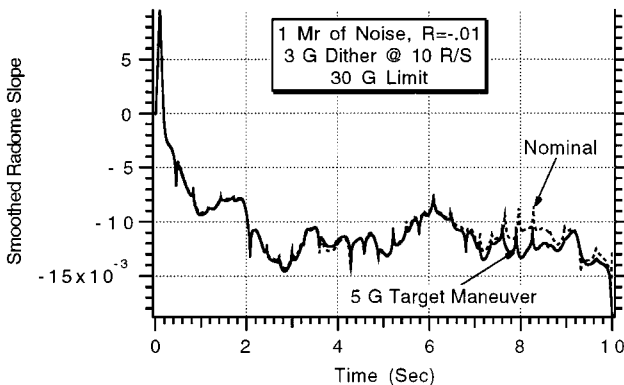


Fig. 17 Larger target maneuver does not degrade radome slope estimation capability.

degraded about 20% but still there was a tremendous improvement over doing nothing at all, i.e., no compensation. In the other set of cases, a 1-g dither and 1-g target maneuver were assumed. In those sets of experiments, the miss with radome compensation showed a significant improvement over using no compensation.

### Using a Kalman Filter

So far we have used common sense and the dither principle in estimating radome slope for the single plane example considered. A Kalman filter can also be used to provide a more systematic framework so that when cross-plane slopes are considered the dithering scheme can logically be extended and the filter states can be augmented. Figure 18 presents an adaptive radome slope compensation scheme in which a Kalman filter is utilized. In this scheme the Kalman filter simply replaces the division in Fig. 9. The use of bandpass filtering is still used to extract useful information from the dither signal. Once the slope is estimated with the Kalman filter, the method of compensation remains the same as the earlier method. The purpose of the Kalman filter is just to estimate the radome slope. Estimates of the line-of-sight rate for guidance purposes can still be accomplished with a simple noise filter, as shown in Fig. 18, or with an additional Kalman filter if so desired.

The plant equation on which the Kalman filter for estimating radome slope is based is shown next where the states considered are line-of-sight angle, line-of-sight rate, and radome slope. This model assumes that the radome slope is a constant, i.e., because its derivative is zero. Process noise is added to the radome slope equation to account for the fact that the slope may not be a constant, that is,

$$\begin{bmatrix} \dot{\lambda} \\ \ddot{\lambda} \\ \dot{R} \end{bmatrix} = \begin{bmatrix} 0 & 1 & 0 \\ 0 & 0 & 0 \\ 0 & 0 & 0 \end{bmatrix} \begin{bmatrix} \lambda \\ \dot{\lambda} \\ R \end{bmatrix} + \begin{bmatrix} 0 \\ 0 \\ u_s \end{bmatrix}$$

Both the systems dynamics matrix and the process noise matrix can be found from the preceding equation. In many applications the measurement noise matrix is either constant or a known function of time. In this particular application the measurement equation is unusual because it contains the body angle  $\theta$ , which is assumed to be known perfectly. Thus,

$$\lambda^* = [1 \ 0 \ -\theta] \begin{bmatrix} \lambda \\ \dot{\lambda} \\ R \end{bmatrix} + u_n$$

Once the Kalman gains  $K_1$ ,  $K_2$ , and  $K_3$  are obtained by solving the Riccati equations, the resultant Kalman filter can be expressed in matrix form as

$$\begin{bmatrix} \dot{\lambda} \\ \ddot{\lambda} \\ \dot{R} \end{bmatrix} = \begin{bmatrix} 0 & 1 & 0 \\ 0 & 0 & 0 \\ 0 & 0 & 0 \end{bmatrix} \begin{bmatrix} \hat{\lambda} \\ \dot{\hat{\lambda}} \\ \hat{R} \end{bmatrix} + \begin{bmatrix} K_1 \\ K_2 \\ K_3 \end{bmatrix} \left[ \lambda^* - [1 \ 0 \ -\theta] \begin{bmatrix} \hat{\lambda} \\ \dot{\hat{\lambda}} \\ \hat{R} \end{bmatrix} \right]$$

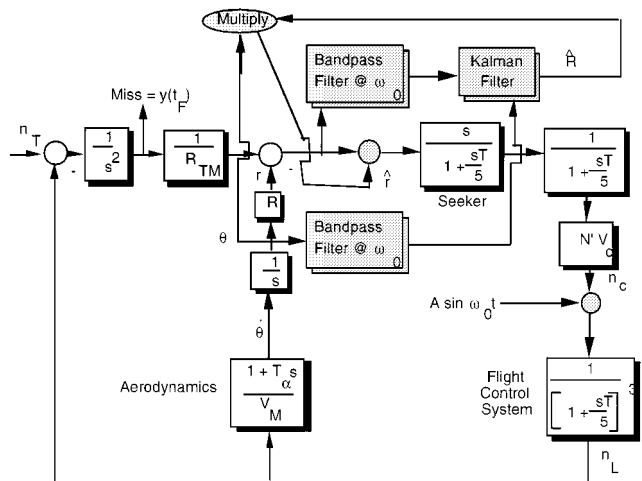


Fig. 18 Adaptive dither scheme with Kalman filter.

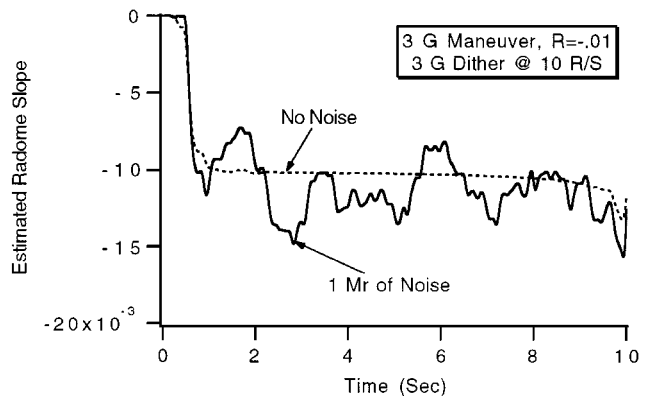


Fig. 19 Kalman filter is able to estimate negative radome slope.

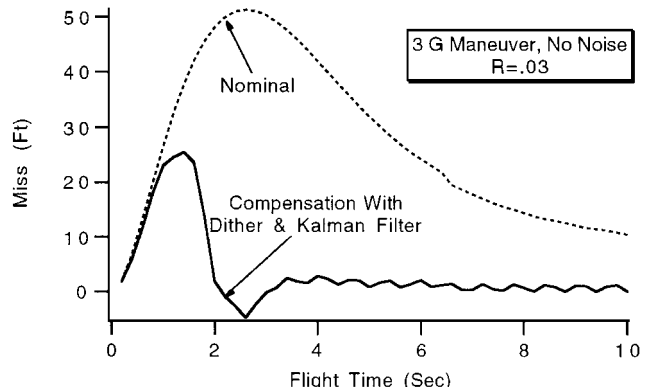


Fig. 20 Dither and compensation using Kalman filter reduces miss due to positive radome slope.

In summary, the preceding equation assumes that the line-of-sight angle is being measured and that the missile body angle is known exactly.

Figure 19 shows that when the Kalman filter is used, negative radome slopes can be estimated accurately, even in the presence of measurement noise. Adjusting the process noise matrix will change the bandwidth of the Kalman filter, which in turn will influence how quickly and accurately the radome slope can be estimated.

Because the radome slope can be accurately estimated with the Kalman filter, it is expected that system performance can be improved. Figure 20 shows how the miss due to a 3-g target maneuver varies with flight time. For flight times less than 10 s the miss can be quite large in the presence of a positive radome slope if no compensation techniques are used. The ability of the Kalman filter to

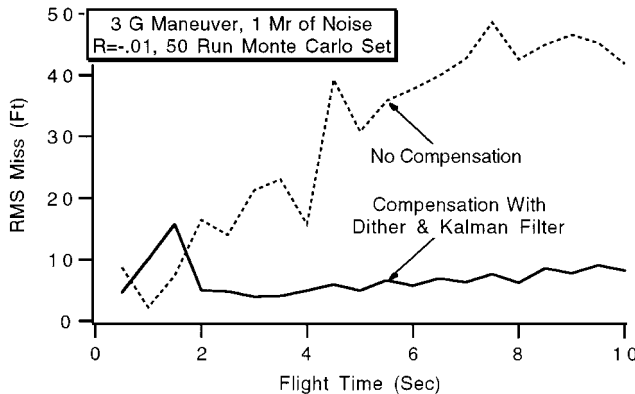


Fig. 21 Dither and compensation with Kalman filter improves noise performance in presence of negative radome slope.

estimate the radome slope enables the miss distance to be dramatically reduced for flight times greater than 1 s.

Figure 21 shows how measurement noise and target maneuver influence system performance in the presence of negative radome slope. The rms miss can be quite large, even for large homing times, if no radome compensation techniques are used. We can see from Fig. 21 that when the dithering technique is used in conjunction with Kalman filtering the rms miss is significantly reduced.

## Conclusions

The paper shows that the radome slope can be estimated by using dithering techniques along with bandpass filtering. The radome slope estimates in conjunction with the missile body angle are used to derive an estimated aberration angle, which is used to compensate the missile guidance system against unwanted aberration angle effects. It also shows how Kalman filtering techniques can be applied to same problem so that the concept considered can be extended to the more realistic case where cross-coupling effects are important.

## References

- <sup>1</sup>Gratt, H., McCowan, W., and Jordan, J., "Adaptive Real-Time Estimation of Radome Slope Errors in RF Missiles," *Proceedings of 4th AIAA Technology Readiness Conference* (Natick, MA), AIAA, Reston, VA, July 1995.
- <sup>2</sup>Nesline, F. W., and Zarchan, P., "Radome Induced Miss Distance in Aerodynamically Controlled Homing Missiles," *Proceedings of AIAA Guidance and Control Conference*, AIAA, New York, 1984.
- <sup>3</sup>Zarchan, P., *Tactical and Strategic Missile Guidance*, 3rd ed., AIAA Progress in Astronautics and Aeronautics, Vol. 176, Reston, VA, 1998, pp. 110-116.
- <sup>4</sup>Lin, C. F., *Modern Navigation, Guidance, and Control Processing*, Prentice-Hall, Englewood Cliffs, NJ, 1991, pp. 520-528.
- <sup>5</sup>Lin, J. M., and Chau, Y. F., "Radome Slope Compensation Using Multiple Model Kalman Filters," *Journal of Guidance, Control, and Dynamics*, Vol. 18, No. 3, 1995, pp. 637-640.
- <sup>6</sup>Stallard, D. V., "A Missile Adaptive Roll Autopilot with a New Dither Principle," *IEEE Transactions on Automatic Control*, Vol. 11, No. 3, 1966, pp. 368-378.